

RESEARCH ARTICLE

Proteomic profiling of antisense-induced exon skipping reveals reversal of pathobiochemical abnormalities in dystrophic mdx diaphragm

Philip Doran¹, Steve D. Wilton², Sue Fletcher² and Kay Ohlendieck¹

¹ Department of Biology, National University of Ireland, Maynooth, Co. Kildare, Ireland

² Centre for Neuromuscular and Neurological Disorders, University of Western Australia, Perth, Australia

Received: May 20, 2008
Revised: August 13, 2008
Accepted: September 9, 2008

The disintegration of the dystrophin–glycoprotein complex represents the initial pathobiochemical insult in Duchenne muscular dystrophy. However, secondary changes in signalling, energy metabolism and ion homeostasis are probably the main factors that eventually cause progressive muscle wasting. Thus, for the proper evaluation of novel therapeutic approaches, it is essential to analyse the reversal of both primary and secondary abnormalities in treated muscles. Antisense oligomer-mediated exon skipping promises functional restoration of the primary deficiency in dystrophin. In this study, an established phosphorodiamidate morpholino oligomer coupled to a cell-penetrating peptide was employed for the specific removal of exon 23 in the mutated mouse dystrophin gene transcript. Using DIGE analysis, we could show the reversal of secondary pathobiochemical abnormalities in the dystrophic diaphragm following exon-23 skipping. In analogy to the restoration of dystrophin, β -dystroglycan and neuronal nitric oxide synthase, the muscular dystrophy-associated differential expression of calsequestrin, adenylate kinase, aldolase, mitochondrial creatine kinase and cvHsp was reversed in treated muscle fibres. Hence, the re-establishment of Dp427 coded by the transcript missing exon 23 has counter-acted dystrophic alterations in Ca^{2+} -handling, nucleotide metabolism, bioenergetic pathways and cellular stress response. This clearly establishes the exon-skipping approach as a realistic treatment strategy for diminishing diverse downstream alterations in dystrophinopathy.

Keywords:

Antisense oligomer / DIGE / Exon skipping / *Mdx* / Muscular dystrophy

1 Introduction

Duchenne muscular dystrophy (DMD) is a lethal genetic disease of childhood that severely affects the integrity of muscle fibres [1]. Dystrophinopathies are characterized by

primary abnormalities in the Dp427 isoform of the membrane cytoskeletal protein dystrophin [2]. Severely progressive DMD and its more benign form, Becker muscular dystrophy (BMD), represent allelic muscle disorders [1]. Various strategies for the therapy of dystrophinopathies and related muscular disorders have been evaluated, including biomedical interventions based on the down-regulation of myostatin or utrophin substitution, pharmacological treatments, myoblast transfer, stem cell therapy and gene transfer approaches [3–10]. None of these experimental strategies have led to a long-lasting abrogation of progressive muscle degeneration. In contrast, the recent application of antisense oligomer-mediated exon skipping

Correspondence: Professor Kay Ohlendieck, Department of Biology, National University of Ireland, Maynooth, Co. Kildare, Ireland

E-mail: kay.ohlendieck@nuim.ie

Fax: +353-1-708-3845

Abbreviations: DMD, Duchenne muscular dystrophy; PMO, phosphorodiamidate morpholino oligomer

for treating muscular dystrophy has shown enormous potential for the functional restoration of the primary deficiency in dystrophin [11–13].

Removal of specific exons from the Dp427 transcript can result in the production of internally shortened dystrophin molecules [14]. In contrast to the amino- and carboxy-terminal regions of full-length dystrophin with essential actin-binding properties and dystroglycan interaction domains, respectively, the central rod domain appears to be less critical for the overall functional integrity of dystrophin [2]. Hence, the exon skipping-mediated creation of shortened in-frame transcripts, not unlike some BMD-associated forms of dystrophin, provides an ideal biomedical tool to overcome the severely dystrophic DMD phenotype [15]. Systemic delivery of a phosphorodiamidate morpholino oligomer (PMO) has been clearly demonstrated to result in the body-wide expression of the dystrophin Dp427 isoform [16, 17]. In this study, an established PMO coupled to a cell-penetrating peptide was employed for the specific removal of exon 23 in the mutated mouse dystrophin gene transcript, whose effectiveness was previously demonstrated by PCR analysis, immunoblotting and immunofluorescence microscopy of dystrophin-positive fibres in exon-skipped muscle [18]. We used the established MDX model of DMD [19–21], because the nonsense mutation in dystrophin exon 23 [22] triggers a severely dystrophic phenotype in their diaphragm muscle [23].

Although it is well established that the molecular disintegration of the dystrophin-associated glycoprotein complex is a primary factor in rendering muscle fibres more susceptible to necrosis [24–26], secondary alterations in signal transduction, energy metabolism, ion homeostasis and excitation-contraction coupling represent the critical secondary events that finally lead to muscular dystrophy [27, 28]. Hence, when new therapeutic strategies for the reversal of dystrophic symptoms are tested, it is crucial not only to determine the effect on the primary deficiency, but also to analyse the reversal of secondary abnormalities in experimentally treated muscles. Previous MS-based proteomic analyses of the dystrophic MDX animal model have shown that a large cohort of proteins with a broad variety of cellular functions show altered expression in dystrophin-deficient fibres [29–33], suggesting a complex molecular pathogenesis downstream of the primary genetic abnormality in dystrophin. The subproteomic study of Ca^{2+} -binding proteins in dystrophic microsomes [31], the proteomic screening of the dystrophic tibialis anterior muscle [29] and the DIGE survey of the dystrophic diaphragm [33] have established a drastically altered density of essential marker proteins, including the luminal Ca^{2+} -binding element calsequestrin, the metabolic enzyme adenylate kinase and the muscle-specific stress protein cvHsp, respectively, in MDX tissues [34].

Here, we show the reversal of these key secondary pathobiochemical abnormalities in the expression profile of markers of Ca^{2+} -homeostasis, nucleotide metabolism and cellular stress response in PMO-treated MDX fibres. The DIGE technique was employed since this method represents

one of the most advanced large-scale high-throughput tools for the proteomic comparison of different sets of soluble protein complements [35]. The reduction in gel-to-gel variations has greatly improved the biochemical evaluation of trends in changed protein expression patterns [36–38] and was therefore the preferred method here to detect altered expression levels in previously established biomarkers of dystrophinopathy [33]. The therapeutic restoration of dystrophin and its associated proteins β -dystroglycan and neuronal nitric oxide synthase, as well as the reversal of the muscular dystrophy-induced differential expression of calsequestrin, adenylate kinase, aldolase, mitochondrial creatine kinase and cvHsp in PMO-treated MDX muscle fibres, establishes the exon skipping approach as a suitable biomedical strategy for rectifying secondary abnormalities in X-linked muscular dystrophy.

2 Materials and methods

2.1 Materials

CyDye DIGE fluor minimal dyes, the 2-D clean-up kit for removal of contaminants prior to IEF, IPG strips of pH 3–10 (linear), IPG buffer of pH 3–10 for IEF, the 2D-Quant kit for the determination of protein concentration in electrophoretic samples, electrophoresis-grade chemicals, CBB protein dye and ACN were obtained from Amersham Biosciences/GE Healthcare (Little Chalfont, Bucks, UK). Sequencing grade-modified trypsin for peptide generation was from Promega (Madison, WI, USA), and a matrix kit containing CHCA and the external peptide MS calibration kit Peptidemix-1 were purchased from Laserbiolabs (Sophia-Antipolis, France). Primary antibodies were obtained from Visionbiosystems Novocastra, Newcastle upon Tyne, UK (mAb NCL-DYS2 to the C-terminus of dystrophin isoform Dp427; mAb 8D5 to β -dystroglycan), Abcam Cambridge, UK (pAb ab21128 to the cardiovascular heat shock protein cvHSP; ab36329 to isocitrate dehydrogenase), Millipore, Bedford, MA, USA (pAb 07-571 to the neuronal nNOS isoform of nitric oxide synthase), Affinity Bioreagents, Golden, CO, USA (mAb VIIIID1₂ to the fast isoform of calsequestrin), Abnova, Heidelberg, Germany (mAb A412-1A3 to the muscle-specific CA3-isoform of carbonic anhydrase) and Santa Cruz Biotechnology, Santa Cruz, CA, USA (ab-sc28785 to adenylate kinase isoform AK1). Secondary antibodies used for immunoblot analysis were obtained from Chemicon International (Temecula, CA, USA). The Zenon Alexa Fluor 488 labelling kit, SuperScript III reverse transcriptase and Trizol reagent were from Invitrogen (Melbourne, Australia). AmpliTaq-Gold DNA polymerase was obtained from Applied Biosystems (Scoresby, Victoria, Australia). Chemiluminescence substrates and protease inhibitors were from Pierce and Warriner (Chester, UK) and Roche Diagnostics (Mannheim, Germany), respectively. Immobilon-NC membranes and C-18 Zip-Tips for desalting were purchased from Millipore.

The presiliconization medium Sigmacote, ultrapure lysine for quenching the DIGE labelling reaction and DNase-I enzyme, as well as all other analytical-grade chemicals were obtained from Sigma Chemical Company (Dorset, UK).

2.2 MDX animal model

An established animal model of DMD is represented by the MDX mouse, which is missing the Dp427 isoform of dystrophin due to a point mutation [22]. Although limb muscles do not exhibit severe fibre degradation [19], the MDX diaphragm is severely dystrophic [23] and was therefore analysed in this study. C57BL/10ScSn^{mdx} inbred mice were purchased from the Animal Resource Centre, Perth and housed at the Animal Care Unit, University of Western Australia, Perth. Animals were kept under standard conditions and all procedures were performed in accordance with the National Health and Medical Research Council of Australia guidelines on the use of animals for scientific experiments, and were approved by the Animal Ethics Committee of the University of Western Australia (approval number 03/100/373).

2.3 Antisense oligomer treatment

The PMO probe PMO-P007 was re-suspended in sterile, purified water at a concentration of 5 mM and stored at 4°C until required [17]. PMO-P007 was diluted in normal saline and warmed to 37°C for 5 min before being delivered to the mice by the intraperitoneal route, at a dosage of 10 mg/kg *per* week, beginning at 3 days of age [18]. The improved design of antisense oligonucleotides, the optimization of their delivery and control experiments have previously been described in detail [11, 14, 16–18]. Sham treated animals were injected with an equivalent volume of normal saline. Mice were weighed weekly to monitor for any effects of the treatment on growth of pups or stable weight in the adults. At 10 wk of age the mice were anaesthetized (sodium pentobarbitone 40 mg/kg) and then euthanized by cervical dislocation. Tissues were dissected and frozen in isopentane cooled by liquid nitrogen. For analysis, frozen samples were transported on dry ice to Dublin and stored at –80°C prior to sample preparation.

2.4 RNA preparation and RT-PCR analysis

To establish successful exon skipping, PCR analysis of the dystrophin transcript from normal, mdx and PMO-treated samples was performed. RNA was isolated from frozen tissue blocks using Trizol reagent (Invitrogen) according to the manufacturer's protocol. RT-PCR was performed on 100 ng of total RNA for 35 cycles of amplification, using 1 U of SuperScript III in a 12.5 µL reaction. Primers amplifying exons 18–26 [16–18] were used at 94°C for 30 s, 55°C annealing for 1 min and 68°C extension for 2 min. One microlitre of the RT-PCR product was used for secondary amplification with 6 min hot start and 30 cycles at 55°C

using AmpliTaq-Gold DNA polymerase according to manufacturer's instructions (Applied Biosystems). Products were fractionated on 2% agarose gels, stained with ethidium bromide and the images captured by a Chemi-Smart 3000 gel documentation system (Vilber Lourmat, Marne La Vallee, France).

2.5 Sample preparation

DIGE analysis was performed with two experimental designs, one with three and the other one with two different biological samples, represented by normal *versus* MDX *versus* MDX-PMO, and MDX *versus* MDX-PMO, respectively. The analysis of crude skeletal muscle preparations by DIGE technology has previously been optimized by our laboratory [33, 39, 40]. For the combined proteomic profiling of all three specimens, 12 individual biological replicates of muscle samples (four Control, four MDX and four PMO), and for the direct comparison of MDX *versus* treated specimens, eight individual muscle samples (four MDX, four MDX-PMO) were quick-frozen in liquid nitrogen and ground up into a fine powder using a pestle and mortar. Fractions were added to lysis buffer (9.5 M Urea, 4% w/v CHAPS, 30 mM Tris-Cl, pH 8.5, 2% ampholytes pH 3–10 and 100 mM DTT). In order to eliminate excessive viscosity due to the presence of DNA, 2 µL of DNase-I (200 U) were added *per* 100 µL of extraction buffer [33]. The suspension was also supplemented with a protease inhibitor cocktail (0.2 mM pepabloc, 1.4 µM pepstatin, 0.15 µM aprotinin, 0.3 µM E-64, 1 µM leupeptin, 0.5 mM soybean trypsin inhibitor, 1 mM EDTA) to avoid proteolytic degradation of muscle proteins, and then incubated for 3 h at room temperature, with gentle vortexing every 10 min for 30 s [40]. The samples were briefly sonicated, on ice, and spun at 20 000 × *g* for 20 min. The protein-containing middle layer was carefully removed and, prior to dye labelling, samples were treated with the 2-D clean-up kit from GE Healthcare and then resuspended in DIGE compatible lysis buffer (9.5 M Urea, 4% w/v Chaps, 30 mM Tris-Cl, pH 8.5). Protein concentration was determined using the 2-D quant kit from GE Healthcare. The pH value was verified and, if needed, was adjusted to pH 8.5.

2.6 DIGE labelling

Samples were labelled with *N*-hydroxy succinimidyl ester derivatives of the cyanine dyes Cy2, Cy3 and Cy5 following a standard protocol [38]. Typically, 50 µg of lysate was minimally labelled with 200 pmol of either Cy3 or Cy5 for comparison on the same 2-D gel [33, 40]. Labelling reactions were performed on ice in the dark for 30 min and then quenched with a 50-fold molar excess of free lysine to dye for 10 min on ice. A pool of all samples was also prepared and labelled with Cy2 to be used as a standard on all gels to aid image matching and crossgel statistical analysis. Typically, 4.17 µg of C1-C4, MDX1-MDX4 and PMO1-PMO4 were labelled with Cy2. To conform to best experimental practice, a randomized

labelling was performed. Four biological replicates from each of the three experimental populations were either labelled with Cy3 or Cy5 minimal dyes. Samples were both evenly distributed between CyDye Fluors and between analytical gels. The labelled protein extracts were pooled and immediately used for electrophoresis. An equal volume of $2 \times$ sample buffer (9.5 M Urea, 4% w/v CHAPS, 2% IPG buffer pH 3–10 and 130 mM DTT) was added and this suspension was left on ice for 10 min prior to electrophoretic separation. For the direct comparison of MDX *versus* MDX-PMO samples, the above protocol was adapted accordingly. As described above, 50 μ g of lysate were minimally labelled with 200 pmol of either Cy3 or Cy5 for comparison on the same 2-D gel, and for the pooled standard, typically 6.25 μ g of MDX1-MDX4 and PMO1-PMO4 were labelled with Cy2.

2.7 Gel electrophoresis

The 2-D gel electrophoretic separation of fluorescently labelled muscle proteins was carried out by standard procedure using the recommended total protein concentration of 150 μ g protein *per* comparative DIGE gel [39]. Using a reswelling tray from GE Healthcare, IPG strips pH 3–10 (linear) were rehydrated for 12 h with 0.45 mL of rehydration buffer (9.5 M urea, 4% w/v CHAPS, 100 mM DTT, 2% ampholytes pH 3–10), which had been complemented with 0.05% bromophenol blue as a tracking dye. Following placement of the first-dimension strips gel-side up into the Ettan IPGphor manifold and coverage with 108 mL of dry strip cover fluid, protein samples were loaded by anodic cup loading and were then run on the IPGphor III IEF system from GE Healthcare. The following IEF gel running conditions were used: 180 min at 300 V (step-and-hold), 180 min at 600 V (gradient), 180 min at 1000 V (gradient), 180 min at 8000 V (gradient), 240 min at 8000 V (step-and-hold), 180 min at 500 V (step-and-hold) and 120 min at 8000 V (step-and hold). Following IEF strips were equilibrated for 15 min in equilibration buffer (6 M Urea, 30% w/v glycerol, 2% w/v SDS, 100 mM Tris-Cl, pH 8.8) containing 100 mM DTT and another 15 min in equilibration buffer supplemented with 0.25 M iodoacetamide. Using the Ettan DALT twelve system from GE Healthcare, the second dimensional separation of muscle proteins was performed with 12.5% resolving gels. Following brief washing in SDS running buffer, IEF strips were positioned on top of the second-dimension slab gel with the help of a 1% w/v agarose sealing gel, poured on top of the strip and left to solidify. Six DIGE gels and two pick gels were run for 0.2 W/gel for 1 h, followed by 0.4 W/gel for 1 h and then ran at 1.5 W/gel overnight until the blue dye front had just disappeared from the bottom of the gel.

2.8 Gel image acquisition and image analysis

Fluorescently labelled proteins were visualized using the Typhoon Trio variable mode imager system from Amersham Biosciences/GE Healthcare. Cy2, Cy3 and Cy5 images were

scanned using a 488, 532 and 633 nm laser, respectively. The PMT value for all scanned images was between 500 and 600 V. All gels were scanned at 100 μ m resolution and, prior to analysis, gel images were cropped using the ImageQuant TL software program [40]. Gel analysis was performed with the DeCyder V6.5 2-D analysis software package for DIGE (Amersham Biosciences/GE Healthcare). The DeCyder differential in-gel analysis module was used for pairwise comparison of each set of differential samples to the pooled standard present in each gel and for the calculation of normalized spot volume/protein abundance. The 18-spot maps corresponding to the six gels were used to calculate average abundance and paired Student's *t*-test *p*-values for each protein across all analytical gels. This was carried out with the DeCyder biological variation analysis module taking into account Cy3/Cy2 and Cy5/Cy2 ratios for each individual protein. Protein spots that showed a significant increase or decrease were then identified using MS fingerprinting analysis.

2.9 Sample preparation for MS analysis

2-D muscle protein spots of interest, electrophoretically separated on Coomassie-stained pick gels parallel to DIGE gels, were washed, digested and identified by MALDI-TOF MS analysis as previously optimized by our laboratory [33, 39, 40]. The gel was first washed with deionized water (two changes, 10 min each). CBB-stained spots of interest were excised from the gels, using a blue pipette tip with the top cut off and placed into a presiliconized (Sigma, Sigmacote) 1.5 mL Eppendorf tubes. The gel plugs were then destained, desalted and washed as follows: gel plugs were first washed with water and 50 mM $\text{NH}_4\text{HCO}_3/\text{ACN}$ 1:1 v/v for 15 min. All remaining liquid was removed, and enough ACN was added to cover the gel plugs. ACN was removed and gel plugs were rehydrated in 50 mM NH_4HCO_3 . After 5 min, an equal volume of ACN was added. Following 15 min of incubation, all the liquid was removed and the gel plugs were then shrunk in ACN. The ACN was removed and gel plugs were dried down for 30 min using a Heto type vacuum centrifuge from Jouan Nordic A/S (Allerod, Denmark). Individual gel plugs were rehydrated in digestion buffer (1 μ g of trypsin in 20 μ L of 50 mM NH_4HCO_3) to cover the gel plugs. More digestion buffer was added if all the initial volume had been absorbed by the gel pieces. The samples were incubated at 37°C for 1 h. The excess enzyme solution was removed and 8 μ L of 50 mM NH_4HCO_3 was added to each plug to keep the gel plugs wet and the samples were then incubated at 37°C overnight. After digestion, the samples were centrifuged at 12 000 $\times g$ for 10 min. The supernatant was carefully removed from each sample and placed into clean and siliconized plastic tubes. The resulting peptides were extracted by three sequential extraction steps each of 30 min duration and a volume of 40 μ L each. The solvent of the first extraction consisted of 50% ACN/0.1% TFA. Extraction was aided by sonication in a Branson 3100 water bath for 30 min.

Samples were then briefly spun down. The solvents for the remaining two extractions were 60% ACN/0.1% TFA and 80% ACN/1% TFA. The combined extracts were concentrated in a vacuum centrifuge and peptides resuspended in 8 μ L of 3% TFA. Samples were stored at -70°C until analysed by MS methodology.

2.10 MALDI-TOF MS analysis

MALDI-TOF tryptic PMF of in-gel digests from normal, dystrophic and PMO-treated muscle protein species was conducted by standard methodology [40]. Tryptic peptides from individual samples were desalted using Millipore C-18 Zip-Tips and eluted onto the sample plate with the matrix solution (5 mg/mL CHCA in 50% v/v ACN/0.1% v/v TFA). Mass spectra were recorded using an Ettan MALDI-TOF Pro-instrument from Amersham Biosciences operating in the positive reflector mode at the following parameters: accelerating voltage 20 kV; and pulsed extraction: on (focus mass 2500). Standard peaks of angiotensin III (897.5 m/z) and ACTH (2465.19 m/z) were used for internal calibration. MALDI evaluation software was used for the analysis of mass spectra and protein identification was achieved with the PMF ProFound search engine for peptide mass fingerprints. All certainty hits of diaphragm muscle proteins generated by the ProFound search engine were matched against the publicly available search engine MASCOT (<http://www.matrixscience.com>).

2.11 Immunoblotting

In order to confirm altered expression levels of distinct diaphragm muscle proteins, as revealed by fluorescence DIGE analysis, 2-D immunoblotting with highly specific primary antibodies was employed [33, 40]. The soluble muscle proteome was electrophoretically separated as described above and then transferred at 100 V for 80 min to Immobilon NC-pure membranes using a Transblot Cell from BioRad Laboratories (Hemel Hempstead, Herts, UK). 2-D blots were blocked in 50 mM sodium phosphate, pH 7.4, 0.9% w/v NaCl, containing 5% w/v fat-free milk powder, followed by exposure to sufficiently diluted primary antibodies, extensive washing, incubation with peroxidase-conjugated secondary antibodies and finally washed again prior to visualization of immunodecorated muscle protein spots. The SuperSignal ECL kit from Pierce and Warriner was used for evaluating antibody labelling intensity and a Typhoon Trio variable mode imager from Amersham Biosciences/GE Healthcare with ImageQuant TL software was used for image acquisition.

2.12 Immunofluorescence microscopy

Microscopical localization of diaphragm proteins was carried out as previously described in detail [18]. Dystrophin, β -dystroglycan and the neuronal nNOS isoform of nitric oxide synthase were detected by antibody labelling in 6 μ m

unfixed transverse cryosections. Immunofluorescence labelling was performed using the Zenon Alexa Fluor 488 labelling kit according to the protocol recommended by the manufacturer, but omitting the initial fixation step. Diaphragm sections were viewed with an Olympus IX-70 inverted microscope and the images captured on an Olympus DP-70 digital camera. Images in each montage were photographed using the same parameters to allow comparison.

3 Results

3.1 Proteomic profiling of antisense-induced exon skipping in dystrophic diaphragm

In order to demonstrate that exposure to PMO resulted in the specific removal of exon 23 in the mutated mouse dystrophin gene transcript, the PCR analysis of transcripts from RNA prepared from normal, MDX and PMO-treated mice is shown in Fig. 1A. The full-length transcript is represented by a 1357 bp product and the exon-23 deleted transcript by a 1144 bp product. Following the establishment of successful exon skipping, which has previously been described in detail by Wilton and coworkers [16–18], immunofluorescence microscopy was used to show the relocation of dystrophin in PMO-treated diaphragm preparations. As illustrated in Fig. 1B, antibody labelling of dystrophin and two of its associated elements, β -dystroglycan and the neuronal nNOS isoform of nitric oxide synthase, showed the surface localization of these proteins in PMO-treated tissue. Since this also agreed with successful exon skipping and established the restoration of essential components of the dystrophin-associated sarcolemma complex, the same diaphragm specimens were used for a subsequent proteomic profiling analysis. Differential labelling with the fluorescent dyes Cy2, Cy3 and Cy5 was carried out with a combination of four biological repeats of normal, MDX and PMO-treated MDX specimens. Figure 2 illustrates the composition of a representative set of six analytical DIGE gels. In our study, we conformed to best experimental practice using the DIGE technique, as reviewed by Friedman and Lilley [41]. A randomized labelling protocol was followed and samples were evenly distributed with respect to CyDye fluor staining and the cohort of analytical gels [35–38]. DIGE analysis of experimental exon-skipping therapy was carried out with two experimental designs. As shown in Figs. 3 and 4, the first approach was performed with three different biological samples, representing normal *versus* MDX *versus* MDX-PMO specimens. In contrast, the second analytical approach focused on two different biological samples, representing MDX *versus* MDX-PMO specimens (Figs. 5 and 6). Subsequently, proteomic findings were validated by comparative immunoblot analysis of key muscle marker proteins, as shown in Fig. 7.

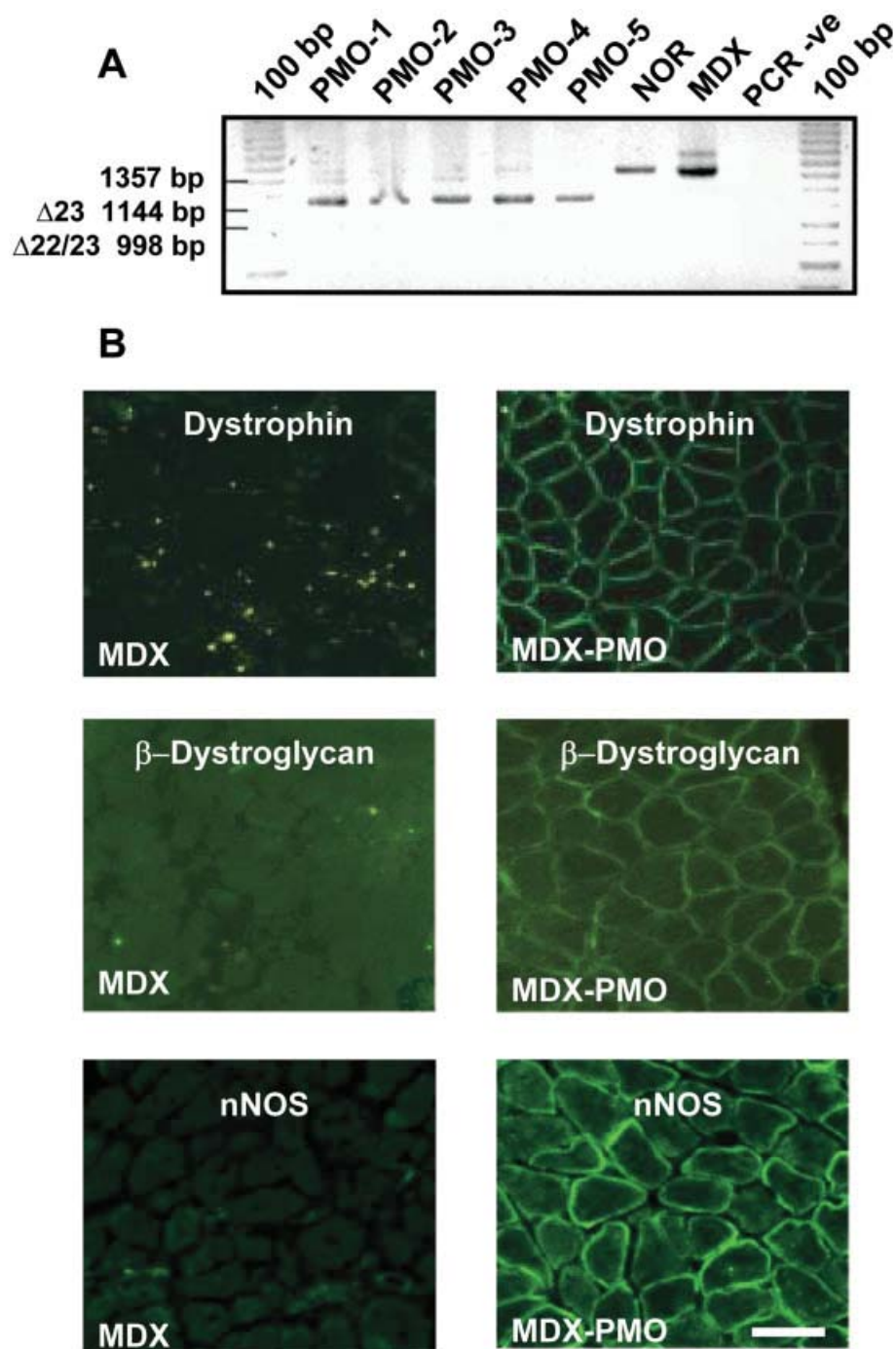


Figure 1. PCR and immunofluorescence analysis of dystrophin in antisense oligomer-treated MDX diaphragm. (A) RT-PCR analysis of normal, MDX and PMO-treated diaphragm tissue. The product of 1357 bp represents the full-length dystrophin transcript, whereas the products of 1144 and 998 bp represent transcripts excluding exon 23, and exons 22 and 23, respectively. PMO-1 to PMO-5 represents preparations from five individual MDX mice treated with antisense oligonucleotides. The outer lanes contain a 100 bp ladder. (B) The restoration of surface expression of dystrophin, β -dystroglycan and the neuronal nNOS isoform of nitric oxide synthase in PMO-treated MDX tissue as compared to untreated MDX diaphragm muscle. Immunofluorescence microscopy was performed with 6 μ m unfixed cryosections. Bar equals 50 μ m.

3.2 Reversal of pathobiochemical abnormalities in dystrophic diaphragm

The proteomic comparison of normal *versus* MDX *versus* PMO-treated MDX specimens is illustrated in the Cy2-labeled DIGE master gel in Fig. 3. Out of approximately 2500 detectable 2-D protein spots, 20 muscle proteins showed a differential expression pattern. The comparative gel electro-

phoretic analysis of the normal *versus* the MDX diaphragm proteome, employing a Typhoon Trio variable imager and DeCyder 2-D analysis software, showed five increased and 15 decreased protein species. The overall 2-D spot pattern of the master gel agrees with our previously published studies on the dystrophic diaphragm muscle [32–34]. Muscle protein species with a changed abundance in MDX diaphragm, ranging in molecular mass from 6.2 kDa (α -globin) to

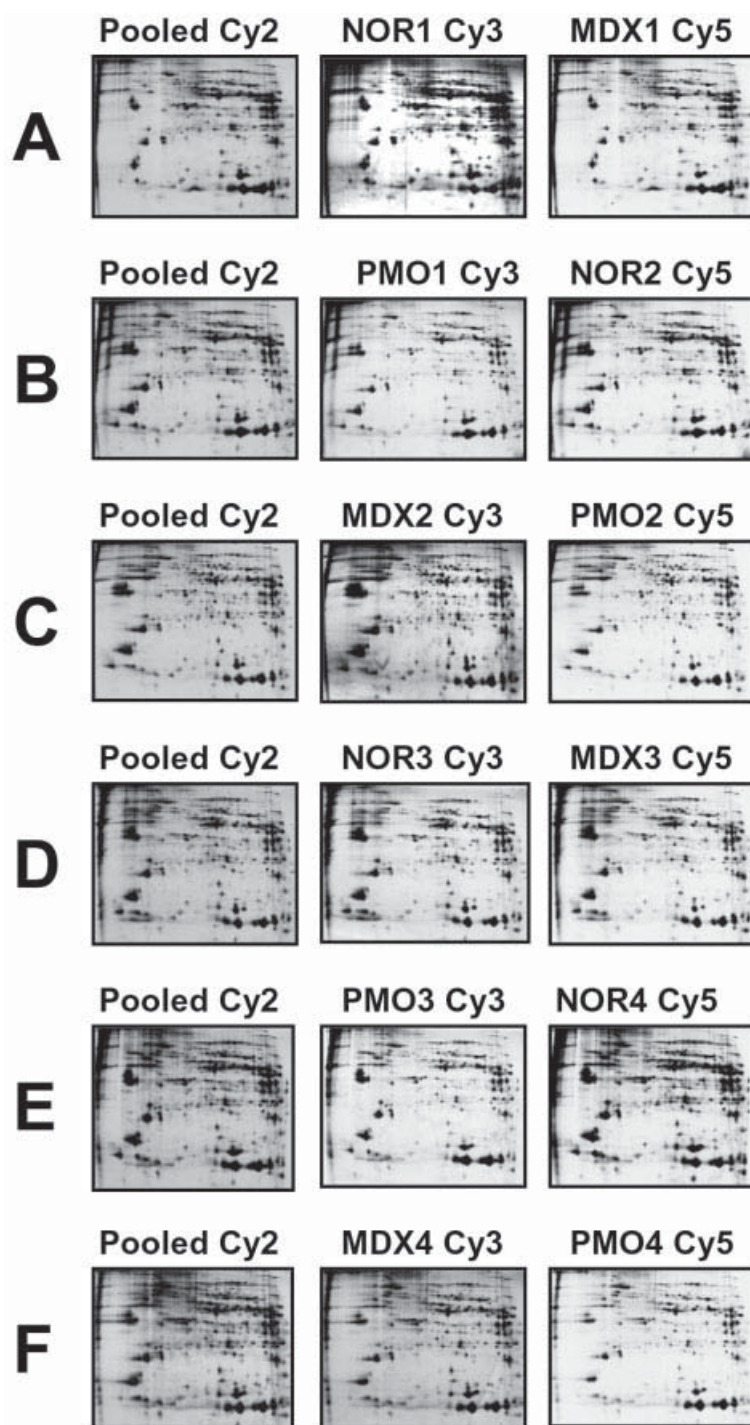


Figure 2. Overview of DIGE analysis of antisense oligonucleotide-induced exon skipping in dystrophic MDX diaphragm. (A–F) The composition of a set of six analytical DIGE gels. To conform to best experimental practice, a randomized labelling protocol was performed. Four sample replicates from each of the three experimental populations (NOR, normal diaphragm; MDX; dystrophic diaphragm; PMO, PMO-treated dystrophic diaphragm) were either labelled with Cy3 or Cy5 minimal dyes. Samples were both evenly distributed between CyDye Fluors and between analytical gels. A pool of all samples was prepared and labelled with Cy2 to be used as a standard on all gels to aid image matching and crossgel statistical analysis.

72.6 kDa (succinate dehydrogenase), covered a *pI* range from *pI* 5.0 (myosin light chain) to *pI* 9.2 (isocitrate dehydrogenase). Table 1 lists the identification of the majority of these proteins using MALDI-TOF MS tryptic PMF from in-gel digests. Diaphragm muscle components with a disturbed expression pattern belonged to the class of cellular components that are involved in muscle contraction, cytoskeleton

formation, mitochondrial function, metabolism, ion homeostasis, and chaperone function. In Fig. 4 are shown expanded views of DIGE gels of the fluorescently labelled normal muscle proteome, the dystrophic protein complement, PMO-treated specimens and pooled standards, as well as the comparative graphic representation of spots representing individual marker proteins. Most importantly, the AK1 iso-

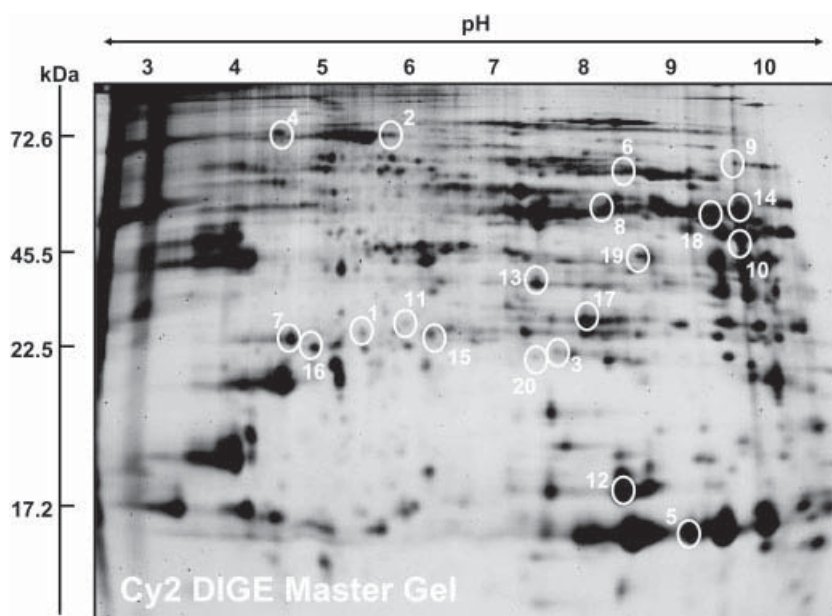


Figure 3. Two-dimensional gel electrophoretic analysis of dystrophic diaphragm following PMO-induced exon skipping. A Cy2-labelled master gel of the total soluble protein complement from normal diaphragm *versus* dystrophic diaphragm *versus* PMO-treated dystrophic diaphragm muscle is shown. Muscle proteins with a differential expression level are marked by circles and are numbered 1–20. See Table 1 for a detailed listing of skeletal muscle proteins with a changed abundance in dystrophic or treated fibres. The pH values of the first dimension gel system and molecular mass standards (in kDa) of the second dimension are indicated on the top and on the left of the panels, respectively.

form of adenylate kinase was confirmed to be reduced in dystrophic fibres as previously reported by Ge *et al.* [29], but this altered expression profile was reversed by PMO-mediated exon skipping. The reduced expression of aldolase and isocitrate dehydrogenase was also partially reversed by PMO application suggesting therapeutic changes in key metabolic steps of glycolysis and the citric acid cycle. In contrast to the reduction in many metabolic enzymes, muscular dystrophy causes a profound upregulation of small stress proteins, such as the muscle-specific heat shock protein cvHsp [33]. The DIGE analysis of this heat shock protein presented in Fig. 3 indicates a less intense stress response in treated MDX fibres.

3.3 Proteomic comparison of MDX *versus* PMO-treated MDX preparations

The direct comparison of MDX *versus* PMO-treated MDX preparation revealed a cohort of 15 protein species with a differential expression pattern. Figure 5A shows a representative master gel of the total soluble protein complement from MDX muscle *versus* PMO-treated dystrophic diaphragm. 2-D gel images with a Cy2-labelled pooled standard, Cy3-labelled dystrophic MDX preparations and Cy5-labelled PMO-treated dystrophic samples are presented in Figs. 5B–D, respectively. Table 2 lists the identification of the majority of these proteins using MALDI-TOF MS tryptic PMF from in-gel digests. In analogy to the above outlined results obtained by the comparison of three biological samples, this analytical approach revealed that muscle proteins with an altered expression level belonged to the class of cellular components that are involved in cytoskeletal activity, glycolysis, mitochondrial function,

metabolic transportation steps, Ca²⁺-homeostasis and chaperone function. Expanded views of DIGE gels of the fluorescently labelled dystrophic protein complement *versus* PMO-treated specimens, as well as the comparative graphic representation of spots representing individual marker proteins, are shown in Fig. 6. An important finding is the changed abundance of cvHsp. Direct comparison of this relatively minor muscle protein in MDX *versus* PMO-treated dystrophic specimens showed a drastic decline in cvHsp density following exon skipping. Hence, the previously reported enhanced cellular stress response and higher cvHsp-related chaperone function in the dystrophic phenotype [33, 42] is being lowered in PMO-treated fibres. In addition, our DIGE-based survey demonstrated that the altered expression profile of adenylate kinase isoform AK1 and the mitochondrial isozyme of creatine kinase in dystrophic fibres were partially reversed by PMO-mediated exon skipping (Fig. 6). Hence, the proteomic data presented here suggest that the modified expression of established markers of secondary dystrophic changes in nucleotide metabolism have been reversed by exon-skipping therapy.

3.4 Immunoblotting confirms exon skipping-induced reversal of dystrophic abnormalities

Verification of proteomic data was carried out by 2-D immunoblot analysis. Dystrophin does not exist in isolation at the muscle surface membrane, but is tightly associated with numerous sarcolemmal proteins, *e.g.* sarcoglycans, dystroglycans, dystrobrevin, syntrophins and sarcospan [43]. Deficiency of the Dp427 isoform results

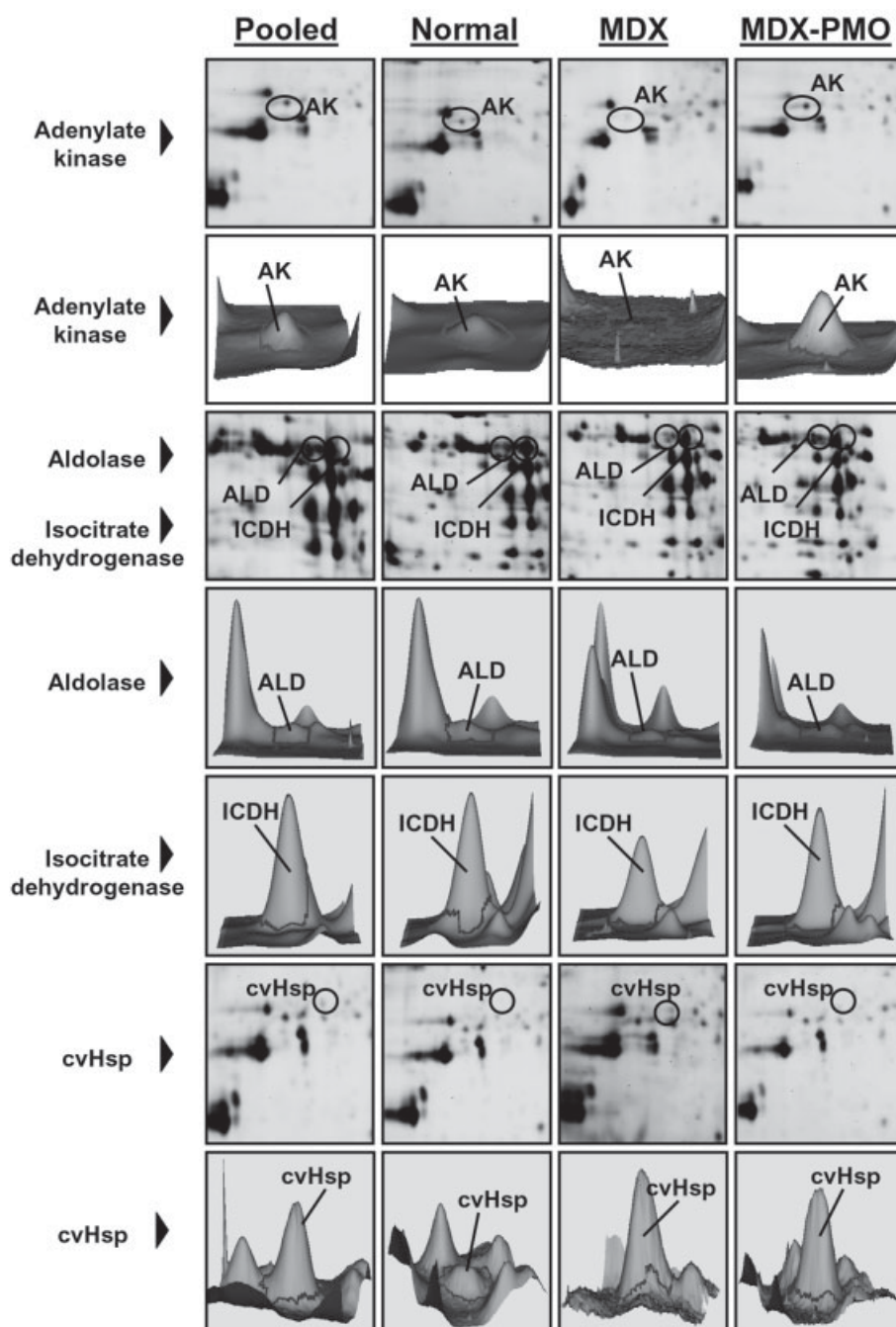


Figure 4. Biochemical status of muscular dystrophy-associated markers in antisense oligomer-treated MDX diaphragm. Expanded views of 2-D gels of the CyDye-labelled samples from normal diaphragm *versus* dystrophic MDX diaphragm *versus* PMO-treated dystrophic diaphragm muscle (MDX-PMO), as well as the comparative graphic representation of protein spots representing adenylate kinase (AK), isocitrate dehydrogenase (ICDH), aldolase (ALD), and the small heat shock protein cvHsp are shown.

in the drastic reduction in most dystrophin-associated proteins [44, 45], it was therefore of interest to determine the effect of exon skipping on the expression of a key element of the dystrophin–glycoprotein complex. As illustrated in Fig. 7, the abundance of β -dystroglycan was drastically elevated following exposure to PMO. Rescued β -dystroglycan expression established that the initial downstream abnormality in dystrophin deficiency is partly rectified in PMO-treated diaphragm. This agrees

with the immunofluorescence analysis shown above in Fig. 1B. Re-establishment of dystrophin is clearly associated with the reappearance of β -dystroglycan and nNOS in the cellular periphery of PMO-treated MDX fibres. Since most peripheral or integral membrane-associated muscle proteins cannot be properly assessed by DIGE methodology, immunoblotting of the Ca^{2+} -binding protein calsequestrin was carried out. A severe reduction in this luminal sarcoplasmic reticulum protein has pre-

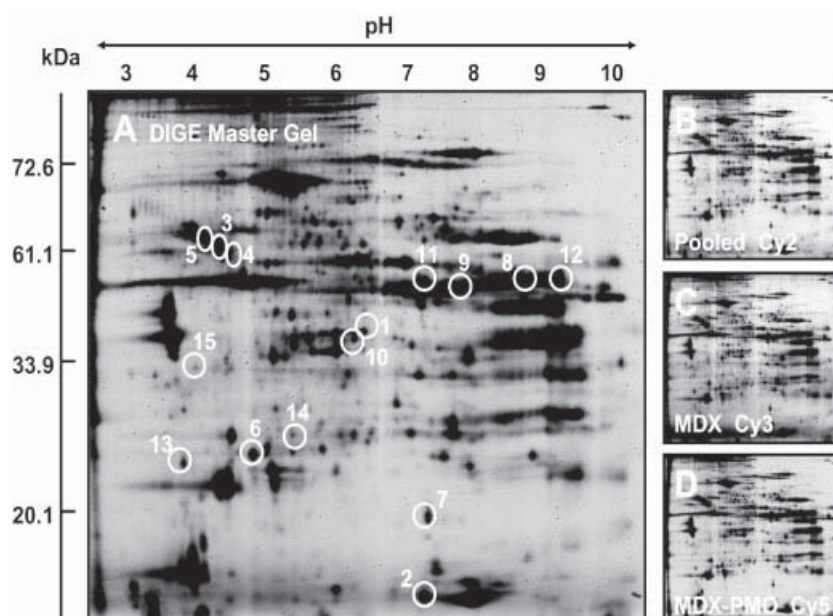


Figure 5. 2-D gel electrophoretic analysis of dystrophic *versus* PMO-treated diaphragm. (A) A Cy2-labelled master gel of the total soluble protein complement from dystrophic diaphragm *versus* PMO-treated dystrophic diaphragm muscle. Muscle proteins with a differential expression level are marked by circles and are numbered 1–15. See Table 2 for a detailed listing of skeletal muscle proteins with a changed abundance in dystrophic or treated fibres. The pH values of the first dimension gel system and molecular mass standards (in kDa) of the second dimension are indicated on the top and on the left of the panels, respectively. (B)–(D) shows representative images of 2-D gels with Cy2-labelled pooled standard, Cy3-labelled dystrophic MDX preparations and Cy5-labelled PMO-treated dystrophic samples (MDX-PMO), respectively.

viously been linked to muscular dystrophy [31]. As shown in Fig. 7, exon skipping appears to restore the expression of this essential ion-handling protein. This suggests that PMO-treatment may at least partially abolish the Ca^{2+} -induced secondary abnormalities in muscular dystrophy. In addition, the immunoblotting of cvHsp, carbonic anhydrase, adenylate kinase and isocitrate dehydrogenase confirmed the findings of the DIGE analysis. The exon-skipping approach appears to reverse abnormal expression levels in a wide range of diaphragm proteins.

4 Discussion

Although the disintegration of the dystrophin-mediated linkage between the extracellular matrix component laminin and the subsarcolemmal actin cytoskeleton is considered the most crucial initial factor in X-linked muscular dystrophy [24], the secondary events rendering a muscle fibre more susceptible to necrosis are not well understood. Recent proteomic surveys have demonstrated that the primary deficiency in the full-length Dp427 isoform of dystrophin and the concomitant loss in dystrophin-associated proteins cause a severely disturbed protein expression pattern in dystrophic muscle fibres [29–33]. The primary molecular collapse of the membrane cytoskeleton seems to trigger altered expression levels for a great variety of muscle proteins involved in diverse cellular functions [34], making the study of the molecular pathogenesis of dystrophinopathy a difficult task. This pathological aspect of muscular dystrophy was clearly confirmed by the analytical findings of this investigation. Changed diaphragm proteins, as identified by DIGE

analysis, can be grouped as muscle components involved in chaperone activity (cvHsp, chaperonine Hsp1, α B crystalline), cytoskeletal function (vimentin, desmin, myotilin), nucleotide metabolism (adenylate kinase, creatine kinase), muscle contraction (myosin light chains), glycolysis (aldolase, triosephosphate isomerase), the citric acid cycle (isocitrate dehydrogenase, succinate dehydrogenase), aldehyde metabolism (aldehyde dehydrogenase), oxygen transport (myoglobin, β -haemoglobin, α -globin), the remethylation pathway of homocysteine homeostasis (betaine-homocysteine methyltransferase), the polyol pathway of glucose metabolism (sorbitol dehydrogenase), cytosolic calcium homeostasis (regucalcin), and the regulation of acid–base balance (carbonic anhydrase).

The proteomic profiling of experimental exon skipping suggests that many of these secondary alterations can be reversed in the MDX animal model. Both, the muscular dystrophy-associated loss of certain metabolic regulators and the compensatory upregulation of chaperones and enzymes can be, at least partially, counter-acted by the specific removal of exon 23 in the mutated mouse dystrophin gene transcript [18]. Previous biochemical studies and more recent proteomic investigations have established an altered status of distinct nondystrophin-related muscle proteins as an integral part of the biomarker signature of X-linked muscular dystrophy [29, 33], besides the primary deficiency in dystrophin and secondary reduction in dystroglycans, sarcoglycans, dystrobrevins, syntrophins and sarcospan [24–26]. For example, pathobiochemical indicators of dystrophinopathy are represented by adenylate kinase, calsequestrin and cvHsp [34]. The determination of their expression levels indi-

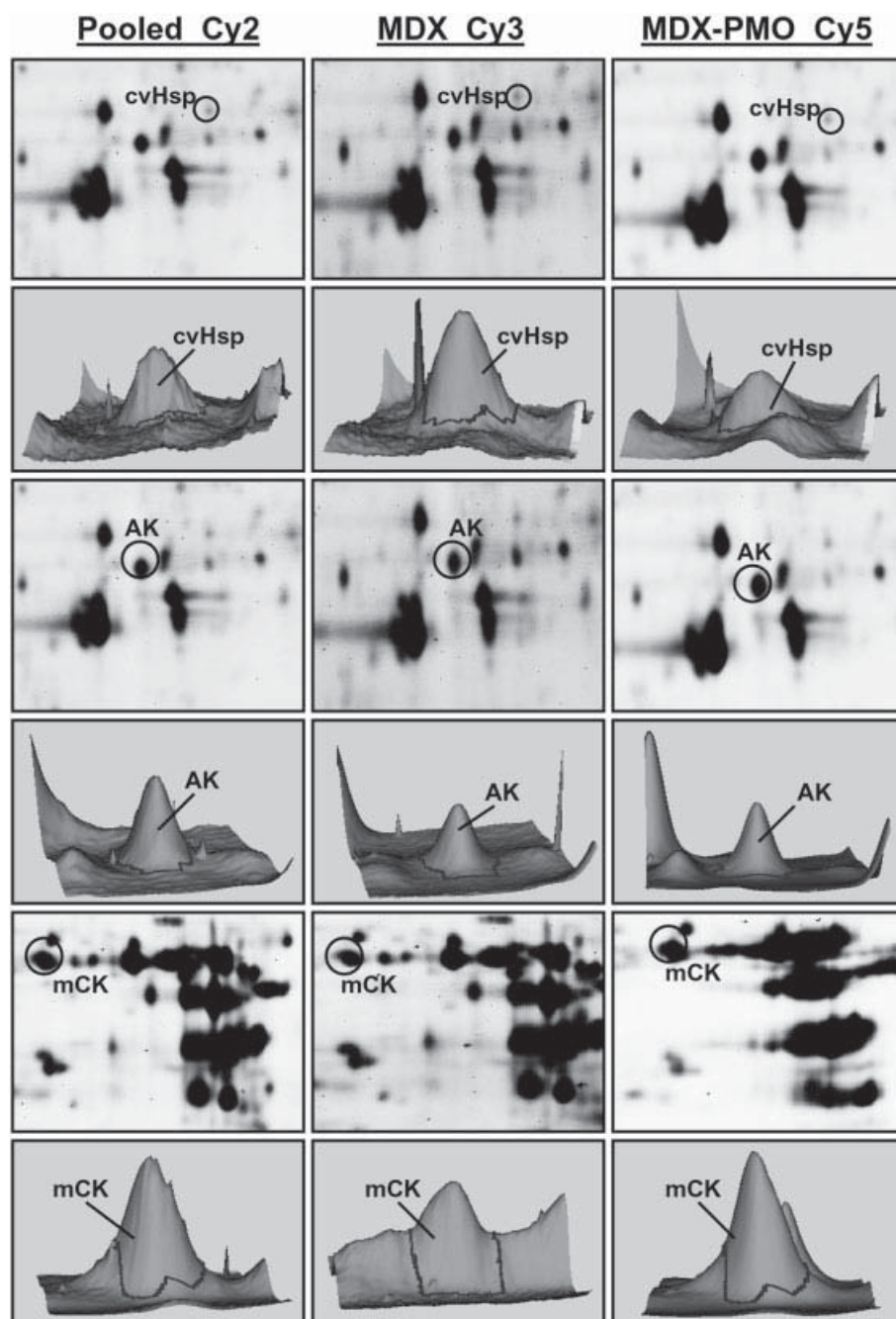


Figure 6. Proteomic profiling of dystrophic *versus* antisense oligomer-treated MDX diaphragm. Expanded views of 2-D gels of the CyDye-labelled samples from dystrophic MDX diaphragm *versus* PMO-treated dystrophic diaphragm muscle (MDX-PMO), as well as the comparative graphic representation of protein spots representing the small heat shock protein cvHsp, adenylate kinase (AK) and the mitochondrial creatine kinase (mCK) are shown.

cates a reversal of secondary dystrophic symptoms following PMO-treatment. A lower density of the AK1 isoform of adenylate kinase was previously observed in both dystrophic limb [29] and diaphragm [33] muscle, triggering a diminished enzyme activity in MDX fibres. The reversal of this decreased enzyme density by exon skipping therapy is an excellent result showing that this novel approach may be useful for successfully treating some of the dystrophin-associated abnormalities in nucleotide metabolism. In normal fibres, creatine kinase

and adenylate kinase provide a major nucleotide pathway [46]. Hence, altered expression levels within this enzyme system may trigger severe disturbances in nucleotide ratios in dystrophin-deficient fibres. Exposure to therapeutic PMO probes appears to rectify this major metabolic defect in muscular dystrophy.

The calcium hypothesis of dystrophinopathy proposes that a causal connection exists between the loss of sarcolemmal integrity and Ca^{2+} -dependent proteolysis of muscle proteins [47–49]. Abnormal ion handling in mechanically

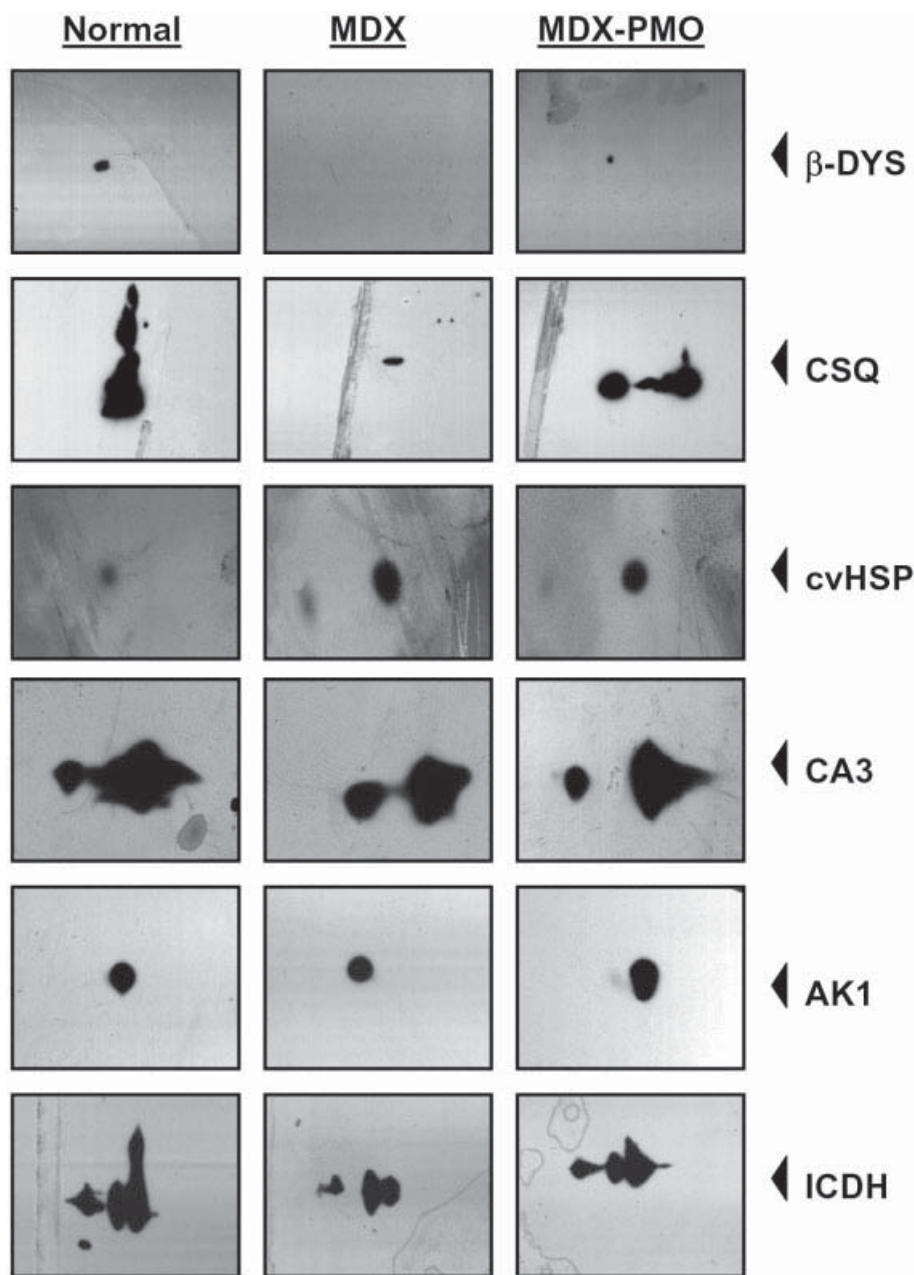


Figure 7. 2-D immunoblot analysis of muscular dystrophy-associated markers in antisense oligomer-treated MDX diaphragm. An expanded view of immunodecorated 2-D spots representing the dystrophin-associated surface glycoprotein β -dystroglycan (β -DG), the sarcoplasmic reticulum Ca^{2+} -binding protein calsequestrin (CSQ), the small heat shock protein cvHsp, carbonic anhydrase isoform CA3, adenylate kinase isoform AK1 and isocitrate dehydrogenase (ICDH) in normal diaphragm *versus* dystrophic MDX diaphragm *versus* PMO-treated dystrophic diaphragm muscle (MDX-PMO) is shown. The position of immuno-decorated spots is marked by arrowheads.

stressed fibres eventually leads to skeletal muscle weakness [50]. Deficiency in dystrophin is clearly associated with the reduced expression of several Ca^{2+} -binding and Ca^{2+} -shuttle proteins [31, 51, 52]. As shown in this study, exon skipping partially restores the expression of calsequestrin in the dystrophic sarcoplasmic reticulum. Consequently, PMO-treatment appears to abolish, at least partially, Ca^{2+} -level associated abnormalities in muscular dystrophy. This is an important finding, since micro-rupturing of the dystrophic plasmalemma has previously been implicated in causing disturbed ion fluxes [53]. However, in contrast to luminal calsequestrin, abnormal expression of the minor cytosolic Ca^{2+} -binding protein rucalgin [32] was shown

not to be affected by exon skipping. Possibly, certain pathological changes due to dystrophin deficiency may cause irreversible damage to distinct protein species, regulatory pathways or signalling mechanism that cannot be rectified using postnatal therapeutic approaches. In addition to the major restoration of calsequestrin, the reversal of the upregulation of the small heat shock protein cvHsp is another indication that exon skipping is a promising new avenue for the treatment of genetic muscle diseases. The upregulation of chaperones such as cvHsp can be considered an autoprotective mechanism of dystrophic fibres in response to large numbers of abnormally folded muscle proteins [42].

Table 1. List of DIGE-identified proteins that exhibit a change of expression in normal *versus* dystrophic MDX *versus* exon skipping-treated MDX-PMO diaphragm muscle

Spot no.	Name of identified proteins	Sequence coverage (%)	Molecular mass (kDa)	pI	Protein accession no.	t-test	Fold change normal vs. MDX	Fold change MDX vs. MDX-PMO	Fold change normal vs. MDX-PMO
1	Heat shock protein cvHSP	20.0	18.66	5.8	gi 6636001	0.00029	+4.28	-1.67	+2.67
2	Succinate dehydrogenase	25.0	72.6	6.8	gi 18426858	0.0085	+1.77	+2.00	+3.53
3	Unknown protein	-	-	-	-	0.0024	+1.70	-1.09	+1.56
4	Unknown protein	-	-	-	-	0.033	+1.65	-1.09	+1.51
5	α -Globin	65.0	6.2	6.8	gi 193761	0.045	+1.61	+1.61	+2.59
6	Aldehyde dehydrogenase	17.7	57.0	7.7	gi 13529509	0.0021	-1.18	+1.53	+1.29
7	Myosin light chain	55.5	22.5	5.0	gi 33563264	0.093	-1.22	-1.36	-1.67
8	Creatine kinase, mitochondrial	30.1	47.9	9.1	gi 38259206	0.0089	-1.36	+1.20	-1.13
9	Myotilin	10.0	55.5	9.2	gi 34879286	0.0044	-1.54	+1.03	-1.50
10	Betaine-homocysteine methyltransferase	19.7	45.5	8.4	gi 62533211	0.008	-1.55	+1.16	-1.33
11	Unknown protein	-	-	-	-	0.0018	-1.61	-1.17	-1.38
12	Myoglobin	20.6	17.2	7.8	gi 11024650	0.048	-1.61	+1.35	-1.19
13	Triosephosphate isomerase	60.0	27.4	6.5	gi 12621074	0.048	-1.65	+1.38	-1.20
14	Isocitrate dehydrogenase	22.0	54.3	9.2	gi 37748684	0.00074	-1.70	+1.05	-1.62
15	Unknown protein	-	-	-	-	0.019	-1.79	-1.05	-1.89
16	Adenylate kinase AK1	31.9	23.3	5.7	gi 10946936	0.0039	-1.84	+1.62	+2.97
17	Carbonic anhydrase CA3	20.3	29.6	6.9	gi 13786200	0.027	-1.86	-1.01	-1.87
18	Aldolase	23.5	39.8	8.9	gi 42490830	0.0045	-1.91	+1.16	-1.65
19	Unknown protein	-	-	-	-	0.0015	-3.04	+1.37	-2.22
20	Unknown protein	-	-	-	-	0.012	-3.31	+1.16	-2.68

The table shows identification, theoretical molecular mass, theoretical pI, percent sequence coverage, fold-change in expression and t-test scores for each of the 20 differentially expressed muscle protein in normal *versus* dystrophic *versus* treated muscle fibres.

Table 2. List of DIGE-identified proteins that exhibit a change of expression in dystrophic MDX *versus* exon skipping-treated MDX-PMO diaphragm muscle

Spot no.	Name of identified proteins	Sequence coverage (%)	Molecular mass (kDa)	pI	Protein accession no.	t-test	Fold change MDX vs. MDX-PMO
1	Unknown protein	-	-	-	-	0.00021	+2.65
2	β -Haemoglobin	54.8	15.8	7.3	gi 229301	0.0032	+2.17
3	Desmin	26.2	53.5	5.2	gi 33563250	0.00021	+2.15
4	Chaperonin Hsp1	22.9	61.1	5.7	gi 31981679	0.00024	+2.12
5	Vimentin	28.7	51.6	4.9	gi 2078001	0.00037	+1.95
6	Adenylate kinase AK1	31.9	23.3	5.7	gi 10946936	0.00064	+1.86
7	α B Crystallin	28.0	20.1	6.8	gi 14789702	0.059	+1.72
8	Aldolase	27.5	39.8	8.9	gi 42490830	0.0013	+1.65
9	Creatine kinase, mitochondrial	30.1	47.9	9.1	gi 38259206	4.4e-005	+1.65
10	Sorbitol dehydrogenase	25.0	40.6	6.6	gi 25108890	0.017	+1.53
11	Creatine kinase	18.9	43.2	6.6	gi 6671762	0.0065	+1.50
12	Isocitrate dehydrogenase	15.0	54.3	9.2	gi 37748684	0.0035	+1.31
13	Unknown protein	-	-	-	-	0.00021	-1.14
14	Heat shock protein cvHSP	21.0	18.66	5.8	gi 6636001	0.00037	-1.92
15	Regucalcin	41.0	33.9	5.2	gi 6677739	4.1e-005	-2.45

The table shows identification, theoretical molecular mass, theoretical pI, percent sequence coverage, fold-change in expression and t-test scores for each of the 15 differentially expressed muscle proteins in dystrophic *versus* treated muscle fibres.

In conclusion, this study has clearly demonstrated that the re-establishment of dystrophin coded by the transcript missing exon 23 diminishes down-stream pathophysiological effects on Ca²⁺-handling, nucleotide metabolism, bioenergetic pathways and cellular stress response. This establishes exon skipping as a suitable therapeutic option for rectifying diverse downstream alterations in dystrophinopathy.

Research was supported by research grants from Muscular Dystrophy Ireland (MDI-125437), Science Foundation Ireland (SFI-04/IN3/B614), National Institutes of Health (RO1NS044146-02), Muscular Dystrophy Association of USA (MDA3718), National Health and Medical Research Council (303216), and infrastructure support from the MHRIF of Western Australia, as well as equipment grants from the Irish Health Research Board (HRB-EQ/2003/3, HRB-EQ/2004/2). We thank Ms Abbie Adams for invaluable technical assistance.

The authors have declared no conflict of interest.

5 References

- [1] Emery, A. E., The muscular dystrophies. *Lancet* 2002, **359**, 687–695.
- [2] Ahn, A. H., Kunkel, L. M., The structural and functional diversity of dystrophin. *Nat. Genet.* 1993, **3**, 283–291.
- [3] Chamberlain, J. S., Gene therapy of muscular dystrophy. *Hum. Mol. Genet.* 2002, **11**, 2355–2362.
- [4] Van Deutekom, J. C., van Ommen, G. J., Advances in Duchenne muscular dystrophy gene therapy. *Nat. Rev. Genet.* 2003, **4**, 774–783.
- [5] Bogdanovich, S., Krag, T. O. B., Barton, E. R., Morris, L. D. *et al.*, Functional improvement of dystrophic muscle by myostatin blockade. *Nature* 2002, **420**, 418–421.
- [6] Partridge, T. A. Myoblast transplantation. *Neuromuscul. Disord.* 2002, **12**, S3–S6.
- [7] Partridge, T. A., Stem cell route to neuromuscular therapies. *Muscle Nerve* 2003, **27**, 133–141.
- [8] Khurana, T. S., Davies, K. E., Pharmacological strategies for muscular dystrophy. *Nat. Rev. Drug Discov.* 2003, **2**, 379–390.
- [9] Mouly, V., Aamiri, A., Perie, S., Mamchaoui, K. *et al.*, Myoblast transfer therapy: Is there any light at the end of the tunnel? *Acta Myol.* 2005, **24**, 128–133.
- [10] Miura, P., Jasmin, B. J., Utrophin upregulation for treating Duchenne or Becker muscular dystrophy: How close are we? *Trends Mol. Med.* 2006, **12**, 122–129.
- [11] Wilton, S. D., Fall, A. M., Harding, P. L., McClorey, G. *et al.*, Antisense oligonucleotide-induced exon skipping across the human dystrophin gene transcript. *Mol. Ther.* 2007, **15**, 1288–1296.
- [12] van Deutekom, J. C., Janson, A. A., Ginjaar, I. B., Frankhuizen, W. S. *et al.*, Local dystrophin restoration with antisense oligonucleotide PRO051. *N. Engl. J. Med.* 2007, **357**, 2677–2686.
- [13] van Ommen, G. J., van Deutekom, J., Aartsma-Rus, A., The therapeutic potential of antisense-mediated exon skipping. *Curr. Opin. Mol. Ther.* 2008, **10**, 140–149.
- [14] Adams, A. M., Harding, P. L., Iversen, P. L., Coleman, C. *et al.*, Antisense oligonucleotide induced exon skipping and the dystrophin gene transcript: Cocktails and chemistries. *BMC Mol. Biol.* 2007, **8**, 57.
- [15] Hoffman, E. P., Skipping toward personalized molecular medicine. *N. Engl. J. Med.* 2007, **357**, 2719–2722.
- [16] Alter, J., Lou, F., Rabinowitz, A., Yin, H. *et al.*, Systemic delivery of morpholino oligonucleotide restores dystrophin expression bodywide and improves dystrophic pathology. *Nat. Med.* 2006, **12**, 175–177.
- [17] Fletcher, S., Honeyman, K., Fall, A. M., Harding, P. L. *et al.*, Dystrophin expression in the mdx mouse after localised and systemic administration of a morpholino antisense oligonucleotide. *J. Gene Med.* 2006, **8**, 207–216.
- [18] Fletcher, S., Honeyman, K., Fall, A. M., Harding, P. L. *et al.*, Morpholino oligomer-mediated exon skipping averts the onset of dystrophic pathology in the mdx mouse. *Mol. Ther.* 2007, **15**, 1587–1592.
- [19] Torres, L. F. B., Duchen, L. W., The mutant mdx: Inherited myopathy in the mouse. *Brain* 1987, **110**, 269–299.
- [20] Watchko, J. F., O'Day, T. L., Hoffman, E. P., Functional characteristics of dystrophic skeletal muscle: Insights from animal models. *J. Appl. Physiol.* 2002, **93**, 407–417.
- [21] Durbeek, M., Campbell, K. P., Muscular dystrophies involving the dystrophin-glycoprotein complex: An overview of current mouse models. *Curr. Opin. Genet. Dev.* 2002, **12**, 349–361.
- [22] Sicinski, P., Geng, Y., Ryder-Cook, A. S., Barnard, E. A. *et al.*, The molecular basis of muscular dystrophy in the mdx mouse: A point mutation. *Science* 1989, **244**, 1578–1580.
- [23] Stedman, H. H., Sweeney, H. L., Shrager, J. B., Maguire, H. C. *et al.*, The mdx mouse diaphragm reproduces the degenerative changes of Duchenne muscular dystrophy. *Nature* 1991, **352**, 536–539.
- [24] Ohlendieck, K., Towards an understanding of the dystrophin-glycoprotein complex: Linkage between the extracellular matrix and the subsarcolemmal membrane cytoskeleton. *Eur. J. Cell Biol.* 1996, **69**, 1–10.
- [25] Cohn, R. D., Campbell, K. P., Molecular basis of muscular dystrophies. *Muscle Nerve* 2000, **23**, 1456–1471.
- [26] Ervasti, J. M., Dystrophin, its interactions with other proteins, and implications for muscular dystrophy. *Biochim. Biophys. Acta* 2007, **1772**, 108–117.
- [27] Deconinck, N., Dan, B., Pathophysiology of Duchenne muscular dystrophy: Current hypotheses. *Pediatr. Neurol.* 2007, **36**, 1–7.
- [28] Batchelor, C. L., Winder, S. J., Sparks, signals and shock absorbers: How dystrophin loss causes muscular dystrophy. *Trends Cell Biol.* 2006, **16**, 198–205.
- [29] Ge, Y., Molloy, M. P., Chamberlain, J. S., Andrews, P. C., Proteomic analysis of mdx skeletal muscle: Great reduction of adenylate kinase 1 expression and enzymatic activity. *Proteomics* 2003, **3**, 1895–1903.
- [30] Ge, Y., Molloy, M. P., Chamberlain, J. S., Andrews, P. C., Differential expression of the skeletal muscle proteome in mdx mice at different ages. *Electrophoresis* 2004, **25**, 2576–2585.

- [31] Doran, P., Dowling, P., Lohan, J., McDonnell, K. *et al.*, Subproteomics analysis of Ca^{2+} -binding proteins demonstrates decreased calsequestrin expression in dystrophic mouse skeletal muscle. *Eur. J. Biochem.* 2004, 271, 3943–3952.
- [32] Doran, P., Dowling, P., Donoghue, P., Buffini, M., Ohlendieck, K., Reduced expression of regucalcin in young and aged mdx diaphragm indicates abnormal cytosolic calcium handling in dystrophin-deficient muscle. *Biochim. Biophys. Acta* 2006, 1764, 773–785.
- [33] Doran, P., Martin, G., Dowling, P., Jockusch, H., Ohlendieck, K., Proteome analysis of the dystrophin-deficient MDX diaphragm reveals a drastic increase in the heat shock protein cHSP . *Proteomics* 2006, 6, 4610–4621.
- [34] Doran, P., Gannon, J., O'Connell, K., Ohlendieck, K., Proteomic profiling of animal models mimicking skeletal muscle disorders. *Proteomics Clin. Appl.* 2007, 1, 1169–1184.
- [35] Unlu, M., Morgan, M. E., Minden, J. S., Difference gel electrophoresis: A single gel method for detecting changes in protein extracts. *Electrophoresis* 1997, 18, 2071–2077.
- [36] Tonge, R., Shaw, J., Middleton, B., Rowlinson, R. *et al.*, Validation and development of fluorescence two-dimensional differential gel electrophoresis proteomics technology. *Proteomics* 2001, 1, 377–396.
- [37] Marouga, R., David, S., Hawkins, E., The development of the DIGE system: 2D fluorescence difference gel analysis technology. *Anal. Bioanal. Chem.* 2005, 382, 669–678.
- [38] Viswanathan, S., Unlu, M., Minden, J. S., Two-dimensional difference gel electrophoresis. *Nat. Protoc.* 2006, 1, 1351–1358.
- [39] Donoghue, P., Doran, P., Wynne, K., Pedersen, K. *et al.*, Proteomic profiling of chronic low-frequency stimulated fast muscle. *Proteomics* 2007, 7, 3417–3430.
- [40] Doran, P., O'Connell, K., Gannon, J., Kavanagh, M., Ohlendieck, K., Opposite pathobiochemical fate of pyruvate kinase and adenylate kinase in aged rat skeletal muscle as revealed by proteomic DIGE analysis. *Proteomics* 2008, 8, 364–377.
- [41] Friedman, D. B., Lilley, K. S., Optimizing the difference gel electrophoresis (DIGE) technology. *Methods Mol. Biol.* 2008, 428, 93–124.
- [42] Nishimura, R. N., Sharp, F. R., Heat shock proteins and neuromuscular disease. *Muscle Nerve* 2005, 32, 693–709.
- [43] Ervasti, J. M., Sonnemann, K. J., Biology of the striated muscle dystrophin-glycoprotein complex. *Int. Rev. Cytol.* 2008, 265, 191–225.
- [44] Ohlendieck, K., Campbell, K. P., Dystrophin-associated proteins are greatly reduced in skeletal muscle from mdx mice. *J. Cell Biol.* 1991, 115, 1685–1694.
- [45] Ohlendieck, K., Matsumura, K., Ionasescu, V. V., Towbin, J. A. *et al.*, Duchenne muscular dystrophy: Deficiency of dystrophin-associated proteins in the sarcolemma. *Neurology* 1993, 43, 795–800.
- [46] Dzeja, P. P., Terzic, A., Phosphotransfer networks and cellular energetics. *J. Exp. Biol.* 2003, 206, 2039–2047.
- [47] Turner, P. R., Westwood, T., Regen, C. M., Steinhardt, R. A., Increased protein degradation results from elevated free calcium levels found in muscle from mdx mice. *Nature* 1988, 335, 735–738.
- [48] Alderton, J. M., Steinhardt, R. A., Calcium influx through calcium leak channels is responsible for the elevated levels of calcium-dependent proteolysis in dystrophic myotubes. *J. Biol. Chem.* 2000, 275, 9452–9460.
- [49] Mallouk, N., Jacquemond, V., Allard, B., Elevated subsarcolemmal Ca^{2+} in mdx mouse skeletal muscle fibres detected with Ca^{2+} -activated K^+ channels. *Proc. Natl. Acad. Sci. USA* 2000, 97, 4950–4955.
- [50] Alderton, J. M., Steinhardt, R. A., How calcium influx through calcium leak channels is responsible for the elevated levels of calcium-dependent proteolysis in dystrophic myotubes. *Trends Cardiovasc. Med.* 2000, 10, 268–272.
- [51] Culligan, K., Banville, N., Dowling, P., Ohlendieck, K., Drastic reduction of calsequestrin-like proteins and impaired calcium binding in dystrophic mdx muscle. *J. Appl. Physiol.* 2002, 92, 435–445.
- [52] Dowling, P., Doran, P., Ohlendieck, K., Drastic reduction of sarcalumenin in Dp427 (dystrophin of 427 kDa)-deficient fibres indicates that abnormal calcium handling plays a key role in muscular dystrophy. *Biochem. J.* 2004, 379, 479–488.
- [53] Clarke, M. S., Khakee, R., McNeil, P. L., Loss of cytoplasmic basic fibroblast growth factor from physiologically wounded myofibers of normal and dystrophic muscle. *J. Cell Sci.* 1993, 106, 121–133.